$U_xM_{1-x}Pt_3$ (M=Y, Lu, In) compounds with the $AuCu_3$ structure

K. Sievers and E.-W. Scheidt
Institut für Physik, Universität Augsburg, Memmingerstrasse 6, D-86135 Augsburg, Germany

G. R. Stewart
Institut für Physik, Universität Augsburg, Memmingerstrasse 6, D-86135 Augsburg, Germany
and Department of Physics, University of Florida, Gainesville, Florida 32611-8440
(Received 12 June 1995)

The nonmagnetic compounds Y-, Lu-, and $InPt_3$ have the $AuCu_3$ structure, which is the cubic stacking of the hexagonal DO19 structure (UPt_3). In order to investigate UPt_3 in this related structure, U was doped onto the M sites in MPt_3 (M=Y, Lu, In); samples retained the $AuCu_3$ structure for up to 40 at. % U. Results of specific-heat and magnetic-susceptibility measurements clearly indicate an enhancement of the electronic density of states at the Fermi level with increasing U concentration. This enhancement is not attributable to single-ion effects but is found to strongly depend on the mean effective U-U distance and not at all on details of the crystal structure. The absence of single-ion effects in dilute UPt_3 in the $AuCu_3$ structure is in contradiction to findings on dilute UPt_3 in DO19 structure. This is discussed as an effect of the different preconditions for f-ligand hybridization in the two related crystal structures.

I. INTRODUCTION

The heavy-fermion system UPt_3 crystallizes in the hexagonal DO19 structure. This crystal structure only differs from the cubic $AuCu_3$ structure in the stacking sequence of the layers. The arrangement of atoms in the close-packed planes is identical in both structures.[1] The DO19 structure appears to favor the formation of a heavy-electron ground state in some way as besides UPt_3 the heavy-fermion systems $CeAl_3$,[2] $UThAl_6$,[3] and $PuGa_3$ (Ref. 4) adopt this structure, too.

Therefore we report here on doping U in nonmagnetic MPt_3 compounds in the $AuCu_3$ structure in order to investigate the role of structure in the origin of the highly correlated electron state in UPt_3. Work on diluted U in DO19 structures [$Th_{(1-x)}U_xAl_3$ (Ref. 3) and $Nb_{(0.65-x)}Zr_{0.35}U_xPt_3$ (Ref. 5)] has already been carried out. In addition to the investigation of the pseudobinary $M_{(1-x)}U_xPt_3$ compounds with M=Y, Lu, In presented in this paper, analogous work has been done and published[6] for $Sn_{(1-x)}U_xPt_3$ showing (unlike the systems discussed here) spin-glass behavior.

II. EXPERIMENTAL AND SAMPLE CHARACTERIZATION

The polycrystalline samples were prepared by arc melting together proper amounts of U (99.95%), Pt (99.99%), and M (typically 99.99%) under a purified, zirconium-gettered argon atmosphere. To ensure homogeneity in composition, each of the alloys was remelted a total of three times with the button turned over between each melting. Samples were checked for weight loss, which was always smaller than 0.5%.

Powder x-ray-diffraction analysis of the as-cast samples showed a single-phase $AuCu_3$ structure without impurity reflections for $(Y,In)_{(1-x)}U_xPt_3$ (x=0.1, 0.2, 0.3) and $Lu_{(1-x)}U_xPt_3$ (x=0.1, 0.2). The compounds $Lu_{0.7}U_{0.3}Pt_3$, $Lu_{0.6}U_{0.4}Pt_3$, and $In_{0.6}U_{0.4}Pt_3$ were obtained as single phase through annealing in a BeO crucible sealed in a Ta crucible. Duration and temperature of the annealing processes are given in Table I. In $M_{(1-x)}U_xPt_3$ compounds with $x>0.4$ (in the case of $Y_{(1-x)}U_xPt_3$ even for $x>0.3$) a secondary phase (UPt_3 in DO19 structure) was detected and could not be eliminated even by different annealing processes; thus the investigation presented here only includes samples containing up to 40 at. % U.

In $(Y,Lu,In)_{(1-x)}U_xPt_3$ the lattice parameter a_0 increases linearly with a small slope with the U concentration x (doping 40 at. % U leads to approximately 1% rise of a_0 starting from values between 4.00 and 4.07 Å). The expansion of a_0 reflects the insertion of the larger U atoms onto M sites in the cubic lattice. It is important to note that with an increase of U concentration both the U-Pt distance $d_{\text{U-Pt}}$ and the mean effective U-U distance $d_{\text{U-U}}$ change. These changes are essential for the discussions below of U-U correlations and hybridization between U $5f$ and Pt $5d/6s$ electrons.

The magnetic dc susceptibility (from 1.65 to 400 K) and magnetization (up to 7 T) measurements were performed in a Quantum Design superconducting quantum interference device magnetometer. Specific-heat measurements from 15 down to 1.25 K were made using a time relaxation method.[7,8]

III. RESULTS AND DISCUSSION

All magnetic susceptibility, magnetization, and specific-heat data presented in this paper are normalized per U mole

TABLE I. Annealed samples with specification of temperature and duration of the annealing process.

Sample	T (°C)	t (h)
$Lu_{0.7}U_{0.3}Pt_3$	1200	168
$Lu_{0.6}U_{0.4}Pt_3$	1200	336
$In_{0.6}U_{0.4}Pt_3$	1000	168

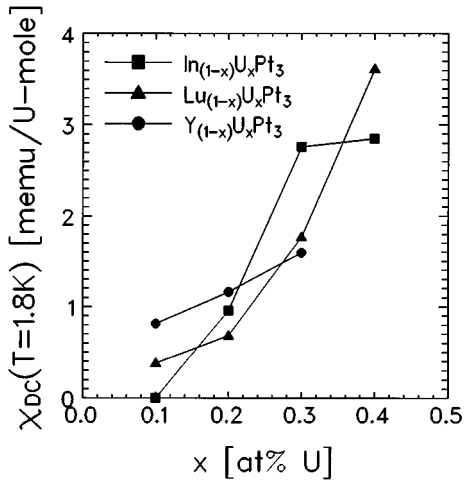

FIG. 1. Magnetic dc susceptibility of $(Y,Lu,In)_{(1-x)}U_xPt_3$ at $T=1.8$ K in $H=5000$ G versus U concentration x. The χ_{dc} values (normalized per U mole) are increasing with x indicative of an enhancement of the electronic density of states dependent upon U concentration.

by subtracting $(1-x)$ times the corresponding quantities for MPt_3 and dividing by x. As the samples $(Y,Lu,In)_{(1-x)}U_xPt_3$ can be referred to as dilute UPt_3 in $AuCu_3$ structure they will be designated as "$AuCu_3$-UPt_3" (as distinguished from DO19-UPt_3) in the following discussion.

The χ_{dc} values per U mole of $(Y,Lu,In)_{(1-x)}U_xPt_3$ at 1.8 K in $H=5000$ G start at below 1 memu/U mole for 10 at. % U and grow to around 3–4 memu/U mole for 40 at. % U. These data are plotted vs U concentration in Fig. 1 and show a stronger increase in χ_{dc} ($T=1.8$ K) with growing U concentration for Lu than for Y, with In showing intermediate behavior.

Specific-heat measurements below 8 K show in a C/T vs T^2 plot a straight line for all samples, which is to say the $C(T)$ data exhibit the behavior of a classical metal: $C(T)=\gamma T+\beta T^3$. Representative low-temperature specific-heat data for $Lu_{(1-x)}U_xPt_3$ are shown in Fig. 2. Plotting the values of the Sommerfeld coefficient γ derived from a fit to

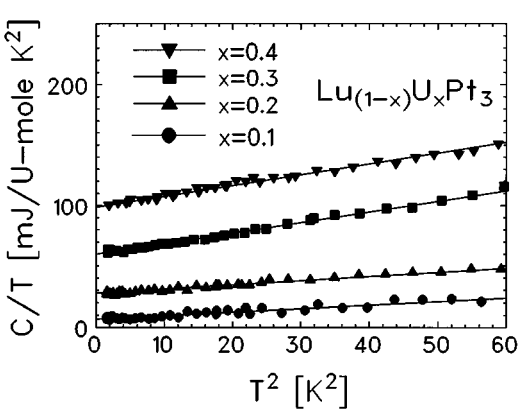

FIG. 2. Specific-heat measurements on $Lu_{(1-x)}U_xPt_3$ plotted as C/T vs T^2; solid lines fit the low-temperature data (1.25 K$\leqslant T\leqslant$8 K) according to $C(T)=\gamma T+\beta T^3$, which gives γ as the intercept on the ordinate.

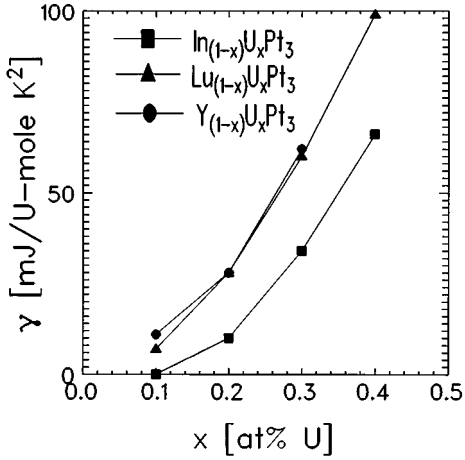

FIG. 3. The Sommerfeld coefficient γ [derived from a fit $C(T)=\gamma T+\beta T^3$ for 1.25 K$\leqslant T\leqslant$8 K] versus U concentration x in $(Y,Lu,In)_{(1-x)}U_xPt_3$. All γ values are normalized per U mole. Increasing U concentration x clearly leads to an enhancement of γ which is proportional to the electronic density of states.

the data versus U concentration x yields a steep rise in γ with x (see Fig. 3) that is, unlike the χ data from Fig. 1, parallel for all three elements Y, Lu, and In.

This pronounced rise in χ_{dc} ($T=1.8$ K) and γ with increasing U concentration in our $AuCu_3$-UPt_3 samples indicates an enhancement of the electronic density of states at the Fermi level $N(E_F)$. The strong dependence upon U concentration of $N(E_F)$, i.e., of χ and γ, rules out single-ion effects as a possible source of the enhancement.

This marked U concentration dependence suggests rather a consideration of the effects of U doping on (1) the mean effective U-U distances $d_{\text{U-U}}$ and (2) the U-Pt distances $d_{\text{U-Pt}}$ in $(Y,Lu,In)_{(1-x)}U_xPt_3$ as possible causes of the enhancement. (3) Another possibility is the changing screening of the f moments due to the differing electronic natures of Y, Lu, and In.

(1) Supposing an ideally statistical distribution of U atoms onto the (Y, Lu, In) sites in the $AuCu_3$ structure the mean effective $d_{\text{U-U}}$ depends on the lattice parameter a_0 and the U concentration x as follows:

$$d_{\text{U-U}}=\sqrt[3]{a_0^3/x}.$$

(2) The closest U-Pt distance $d_{\text{U-Pt}}$ in $AuCu_3$-UPt_3 is computed by the formula

$$d_{\text{U-Pt}}=(\sqrt{2}/2)*a_0.$$

Figure 4 shows $d_{\text{U-U}}$ and $d_{\text{U-Pt}}$ in $AuCu_3$-UPt_3 versus U concentration in comparison to the corresponding quantities in DO19-UPt_3. As is readily visible in Fig. 4, the above inverse cube root dependence of $d_{\text{U-U}}$ on U-U concentration gives a rapid change of the average U-U separation from almost 9 Å at 10 at. % U to 5.5 Å for 40 at. % U. As is to be expected from the small changes of the lattice parameter with U doping the relative change in $d_{\text{U-Pt}}$ with U concentration in $AuCu_3$-UPt_3 is very small compared to the rapid change in $d_{\text{U-U}}$.

Now, let us consider how the $d_{\text{U-U}}$ and $d_{\text{U-Pt}}$ data in Fig. 4 for our $AuCu_3$-UPt_3 samples can be used to understand the χ and γ data. That the weakening of hybridization between U

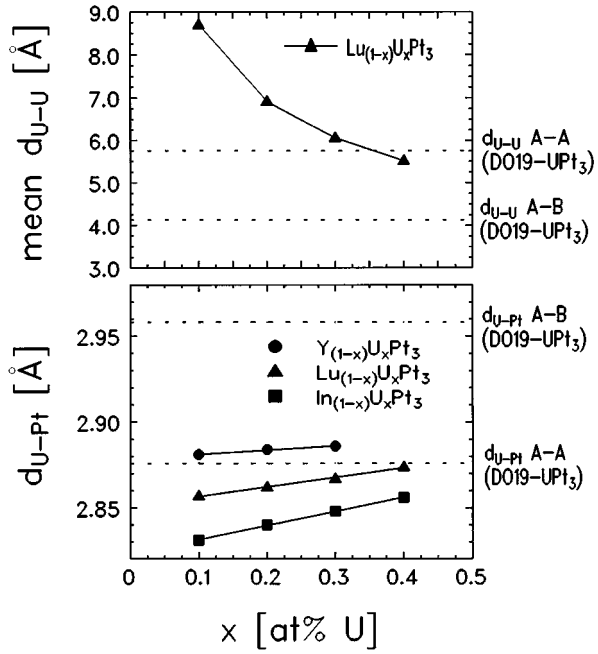

FIG. 4. On regarding $d_{\text{U-U}}$ and $d_{\text{U-Pt}}$ in hexagonal DO19-UPt_3 one has to distinguish carefully between spacings separating atoms within one atomic layer and spacings separating atoms out of consecutive layers. Concerning $d_{\text{U-Pt}}$ this distinction is superfluous for $AuCu_3$-UPt_3 whose cubic symmetry equalizes the different spacings. This is not true for $d_{\text{U-U}}$ in $AuCu_3$-UPt_3 but as the U atoms are assumed to be distributed randomly onto the M sites only the mean $d_{\text{U-U}}$ is regarded to be relevant to U-U correlations. This figure shows the dependence of the mean $d_{\text{U-U}}$ and $d_{\text{U-Pt}}$ upon U concentration x in $(\text{Y,Lu,In})_{(1-x)}U_xPt_3$. For reasons of clarity $d_{\text{U-U}}$ is plotted only for $Lu_{(1-x)}U_xPt_3$ as the corresponding values in $(\text{Y,In})_{(1-x)}U_xPt_3$ differ about less than 1%. The dotted horizontal lines represent the corresponding quantities in pure DO19-UPt_3. $d_{\text{U-U(U-Pt)}}$ A-A labels the U-U (U-Pt) distance within one atomic layer, $d_{\text{U-U(U-Pt)}}$ A-B labels the U-U (U-Pt) distance between atoms out of consecutive layers for DO19-UPt_3.

$5f$ and Pt $5d/6s$ electrons due to the small increase in $d_{\text{U-Pt}}$ is responsible for the enhancement of $N(E_F)$ can be essentially ruled out by the following argument. $d_{\text{U-Pt}}$ in $Y_{0.9}U_{0.1}Pt_3$ is, with a value of 2.88 Å, only slightly greater than $d_{\text{U-Pt}}$ in $Lu_{0.6}U_{0.4}Pt_3$ with 2.87 Å (see Fig. 4). Nevertheless the Sommerfeld coefficient γ [$\propto N(E_F)$]=100 mJ/(U mole K^2) of $Lu_{0.6}U_{0.4}Pt_3$ exceeds the one of $Y_{0.9}U_{0.1}Pt_3$ [γ=11 mJ/(U mole K^2)] by far (see Fig. 3). Hence the mean effective U-U distance $d_{\text{U-U}}$ (rapidly decreasing with increasing U concentration x), and not $d_{\text{U-Pt}}$, seems to control the enhancement of γ in $(\text{Y,Lu,In})_{(1-x)}U_xPt_3$, and, at the minimum, to strongly influence the increase in χ_{dc}. The decreasing $d_{\text{U-U}}$ causes increased U-U correlations. These increased correlations then give rise to the observed monotonic enhancement of γ as shown in Fig. 3. An indication of rising U-U correlations accompanying the decreasing separation of the U atoms can be found in the magnetization. Magnetization measurements on $(\text{Y,Lu,In})_{(1-x)}U_xPt_3$ at T=2 K reveal a decreasing deviation of $M(H)$ from linearity at high fields with increasing U concentration x (see Fig. 5). This decreasing deviation with U concentration may originate from more and more stabilized (antiferromagnetic) correlations between the U atoms

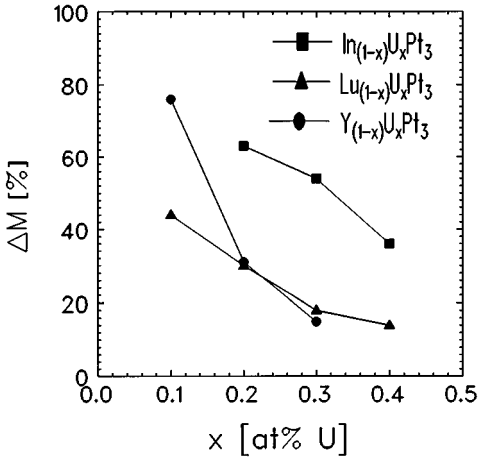

FIG. 5. The deviation of the magnetization from linearity (normalized per U mole) of $(\text{Y,Lu,In})_{(1-x)}U_xPt_3$ at T=2 K in H=7 T versus U concentration x. Increasing U concentration x obviously reduces the deviation. [The value for $In_{0.9}U_{0.1}Pt_3$ is not given because there is no measurable change in its $M(H)$ compared with $M(H)$ of $InPt_3$.]

caused by the shrinking $d_{\text{U-U}}$. However, at least the differences in the behavior of χ_{dc} (T=1.8 K) and M vs H as a function of concentration for the various elements Y, Lu, and In may be ascribable to changes in screening of the f moments by the differing non-f-ligand outer electrons.

Let us now focus on the specific-heat γ values. The γ values as a function of at. % U from Fig. 3 are replotted in Fig. 6 as a function of the calculated $d_{\text{U-U}}$ values. It is clear that extrapolating in Fig. 6 the γ values of $AuCu_3$-UPt_3 versus $d_{\text{U-U}}$ to the value in pure DO19-UPt_3, 4.1 Å, gives a quite startling result: the expected value for γ in the $AuCu_3$ structure for UPt_3 is, within some margin of uncertainty, the same as in the DO19 structure. We therefore conclude that, at

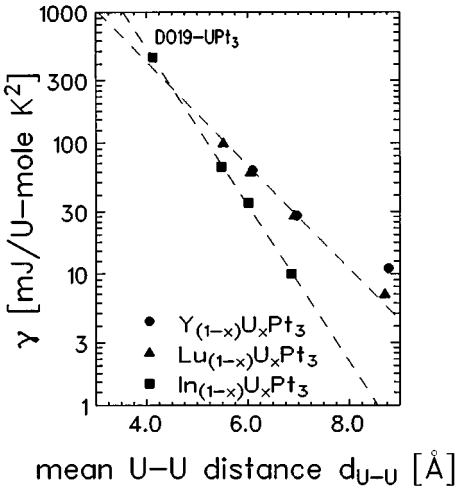

FIG. 6. Logarithm of the Sommerfeld coefficient γ versus mean U-U distance $d_{\text{U-U}}$ in $(\text{Y,Lu,In})_{(1-x)}U_xPt_3$. While the mean $d_{\text{U-U}}$ in $AuCu_3$-UPt_3 is approaching the nearest $d_{\text{U-U}}$ in DO19-UPt_3 (=4.13 Å) also γ in $AuCu_3$-UPt_3 appears to tend towards the high γ of DO19-UPt_3 (dotted lines serve as guide to the eye). The $d_{\text{U-U}}$-γ coordinate of DO19-UPt_3 is marked in the upper left corner of the plot.

least for UPt_3, the large specific heat γ is a strong function of $d_{\text{U-U}}$ and not at all strongly dependent on the details of the hexagonal DO19 crystal structure. The apparent dependence on the mean $d_{\text{U-U}}$ must be operating through the x dependence of the number of pairs of U atoms (or larger clusters) at "first-neighbor" or "second-neighbor" spacings where these terms mean within the A sublattice of the AB_3 structure of $(\text{Y,Lu,In})_{(1-x)}\text{U}_x\text{Pt}_3$. This result is all the more interesting because it apparently contradicts the case of UAl_3 in the DO19 structure [DO19 $Th_{0.5}U_{0.5}Al_3$ has γ=360 mJ/(U mole K^2) (Ref. 3)] compared to the $AuCu_3$ structure [pure UAl_3 occurs in the $AuCu_3$ structure with γ=42 mJ/mole K^2 (Ref. 9)], where the DO19 structure was found to have a much higher γ. This difference with the present work merits further investigation.

One may ask in the present work, why is there no single-ion regime for γ as a function of U concentration, i.e., why is there no regime of "x" where the γ/U mole is finite and constant? Certainly in dilute DO19-UPt_3 [$Nb_{(0.65-x)}U_xZr_{0.35}Pt_3$ (Ref. 5)], γ is constant at about 200 mJ/(U mole K^2) for $0<x\leqslant 0.14$. In cubic UBe_{13} γ is constant [for dilute $M_{(1-x)}U_xBe_{13}$ (Ref. 10)] at about 40% of γ (pure UBe_{13}) for dilutants M smaller than U and shows no single-ion effect for dilutants larger than U. How may we understand the various results?

In the case of $AuCu_3$-UPt_3, the U atoms have 12 nearest Pt neighbors at a similar distance (see Fig. 4) to the only six nearest Pt neighbors to the U in the DO19 structure, while the next-nearest Pt neighbors in this latter structure are somewhat further away. Thus, in $AuCu_3$-UPt_3 the U site is hybridizing with a higher density of Pt s and d electrons than in the DO19 structure; this higher density of electrons available for hybridization leads to a stronger delocalization of U $5f$ electrons establishing comparatively wider $5f$ bands with a low electronic density of states. Thus, above a certain amount of hybridization no large γ due to single-ion effects is formed. In addition to the higher Pt coordination in $AuCu_3$-UPt_3 (which is certainly the decisive factor for the strength of f-ligand hybridization) also the different stacking sequence of atomic layers ($ABAB$ in DO19 and $ABCABC$ in $AuCu_3$ structure) might lead to an unequal effectiveness of f-ligand hybridization. This leaves unanswered the result in $M_{(1-x)}U_xBe_{13}$ for M larger than U, where increasing U-Be ligand distance destroys any single-ion γ.

IV. CONCLUSION

Our studies on dilute UPt_3 in $AuCu_3$ structure [$(\text{Y,Lu,In})_{(1-x)}U_xPt_3$; $0.1\leqslant x\leqslant 0.4$] suggest that in UPt_3 details of the hexagonal DO19 structure play only a minor role for the enhancement of the electronic density of states. This enhancement is in the present work not due to single-ion effects but rather due to U-U correlations; the enhancement appears to be controlled entirely by the mean effective U-U distance. Thus, the γ for $AuCu_3$-UPt_3 extrapolated to the same $d_{\text{U-U}}$ as for DO19-UPt_3 is found to be approximately the same as the 450 mJ/(U mole K^2) observed for pure UPt_3.

The absence of single-ion effects seems to depend on the geometry of the crystal structure: the U-Pt hybridization is intensified by the higher Pt coordination of U atoms in $AuCu_3$-UPt_3 (compared to DO19-UPt_3). The resulting suppression of single-ion effects in $AuCu_3$-UPt_3 is due to the higher degree of delocalization of U $5f$ electrons.

ACKNOWLEDGMENTS

We would like to thank K. Samwer and colleagues for the use of their diffractometer. This work was supported by the Deutsche Forschungsgemeinschaft. Work in Florida was supported by the U.S. Department of Energy under Grant No. DE-FG05-86ER45268.

[1] Charles Barret and T. B. Massalski, *Structure of Metals* (Pergamon, Oxford, 1992), p. 277.

[2] K. Andres, J. E. Graebner, and H. R. Ott, Phys. Rev. Lett. **35**, 1779 (1975).

[3] A. L. Giorgi, G. R. Stewart, M. S. Wire, and J. O. Willis, Phys. Rev. B **32**, 3010 (1985).

[4] G. R. Stewart, B. Andraka, and R. G. Haire, J. Alloys Compounds **213/214**, 111 (1994).

[5] G. Fraunberger, M. Baldus, and G. R. Stewart, Phys. Rev. B **47**, 3204 (1993).

[6] K. Sievers, E.-W-Scheidt, and G. R. Stewart, Physica B**206&207**, 433 (1995).

[7] R. Bachmann, F. J. Di Salvo, T. H. Geballe, R. L. Greene, R. E. Howard, C. N. King, H. C. Kirsch, K. N. Lee, R. E. Schwall, H. U. Thomas, and R. B. Zubeck, Rev. Sci. Instrum. **43**, 205 (1972).

[8] G. R. Stewart, Rev. Sci. Instrum. **54**, 1 (1983).

[9] M. H. Van Maaren, H. J. Van Daal, and K. H. J. Buschow, Solid State Commun. **14**, 145 (1974).

[10] J. S. Kim, B. Andraka, C. S. Jee, S. B. Roy, and G. R. Stewart, Phys. Rev. B **41**, 11 073 (1990).